Ground-state potential curves for Al_2 and Al_2^{6+} in the repulsive region

Nora H. Sabelli*
Chemistry Division, Argonne National Laboratory, Argonne, Illinois 60439

R. Benedek
Materials Science Division, Argonne National Laboratory, Argonne, Illinois 60439

T. L. Gilbert†
Solid State Science Division, Argonne National Laboratory, Argonne, Illinois 60439
(Received 22 December 1978)

Self-consistent-field (SCF) calculations have been performed for the short-range interaction between two aluminum atoms. The ground-state potential curve ($^3\Sigma_g^- \rightarrow {}^5\Sigma_u^- \rightarrow {}^3\Sigma_u^+ \rightarrow {}^1\Sigma_g^+ \rightarrow {}^3\Pi_g$) is presented for internuclear separations between R_e and 0.1 a.u. (repulsive energies up to $\sim 10^3$ a.u.). Basis sets consist of scaled even-tempered Slater orbitals of double-ζ quality, augmented by diffuse functions, with the addition of united or semiunited atom-basis sets centered on the bond. The SCF potentials are compared with Thomas-Fermi theory and with the electron-gas calculations of Wilson, Haggmark, and Biersack. A kink in the SCF screening function is found near $R = 2$ a.u. This feature is believed related to changes in the ground-state configuration that occur in this region. Additional calculations (SCF and linear combination of atomic orbitals) were performed on Al_2^{6+} to determine individually the core overlap and the valence-electron contributions to the interatomic potential. The core-overlap interaction is compared with Gordon-Kim electron-gas calculations. Schematic calculations were also performed on the Al-Al^{3+} system to estimate the interaction between an atom and an energetic ion.

I. INTRODUCTION

To describe the behavior of energetic ions in matter, one requires a theory of both the scattering that results from close atomic encounters and the inelastic processes associated with electronic excitations. To treat both phenomena, the energetic particle is usually considered to undergo a sequence of diatomic collisions. Although in general the interactions are different in a solid than in free space, calculations are normally formulated in terms of diatomic interactions in free space. Early work was based on Thomas-Fermi (TF) atoms.[1,2] The unrealistic long-range behavior of the TF screening function can be improved somewhat by the modifications suggested by Lenz and Jensen[3(a)] and by Moliere.[3(b)]

As a result of painstaking experimental work during the past two decades on particle scattering, range profiles, stopping powers and radiation damage, a need has developed for more fundamental theories of diatomic interactions. Wilson *et al.*[4] (WHB) have used a density-functional approach based on Hartree-Fock-Slater atomic orbitals to calculate short-range interatomic interactions. They obtained potentials that are more strongly screened than either TF or Moliere potentials. Hartree-Fock self-consistent-field (SCF) calculations for short-range diatomic interactions have been performed in a few cases.[5,6] It is of interest to compare results obtained by the density-functional method with SCF calculations, at least for some representative systems.

In the present paper we report on SCF calculations for Al_2, which complement our earlier work on AlH.[6] We consider internuclear separations R that range from the equilibrium value R_e down to 0.1 a.u., which corresponds essentially to the united-atom limit.

As discussed earlier,[6] the strongly repulsive region of the interatomic potential can be calculated by SCF techniques to an accuracy of better than 1%; configuration-interaction calculations for Al_2, AlH, and other Al-based systems for internuclear separations in the vicinity of R_e are currently in progress.

To allow estimates of the relative contribution of valence and core electrons to the interatomic potential, linear combinations of atomic orbitals (LCAO) calculations were performed on the Al_2^{6+} system. By comparing the results of these calculations with SCF calculations for Al_2, the fraction of the total interatomic potential that is due to core overlap can be determined. The core-overlap potential obtained in the above manner will also be compared with approximate closed-shell theories.[7,8]

LCAO calculations for Al_2^{3+} have been performed to give a rough estimate of the effect of the charge state on the interatomic potential in an ion-atom

collision.

The correlation diagrams that are obtained by SCF calculations are of importance to the understanding of inelastic processes associated with electron promotion[9]; however, we do not pursue this application in the present paper.

In Sec. II, we describe the method employed in the SCF calculations and particularly the rationale for the selection of basis functions. The results of the calculations are present and discussed in Sec. III. Finally, some conclusions are stated in Sec. IV.

II. METHOD

For internuclear separations R in the vicinity of R_e, the environment of the valence electrons is quite sensitive to R, whereas the environment of the core electrons is relatively constant.[10] In basis-set expansion calculations, optimization of the exponents at every point would be too costly and therefore the selected basis set must be sufficiently flexible to accomodate the changing environment of the valence electrons. To accomplish this, diffuse and polarization functions are added to atomic basis sets; this procedure enables an accurate description of the bond electrons.

As much smaller separations ($R \ll R_e$) are considered, the united-atom limit is approached, and interpenetration of the core shells occurs. In this region the inner electrons experience a changing environment, whereas the outer electrons acquire a united-atom character. In a basis-set expansion framework, this situation can be represented by united- or semiunited-atom basis sets centered at the midpoint between the nuclei in combination with atomic basis sets centered on the nuclei.

The basis sets employed in the present work and their range of applicability are indicated schematically in Fig. 1. At each separation the selected basis set corresponds to the extent of interpenetration of the atomic shells of Al.

As the internuclear spacing becomes smaller, the overlap between basis functions increases and eventually the set becomes overdetermined. By systematically eliminating the most diffuse atom-centered functions[5(b)] when the overlap becomes too large, we avoid numerical instabilities. The above procedures constitute a straightforward prescription for the selection of basis sets with similar accuracy for $0 < R \lesssim R_e$.

We have employed throughout this work double-ζ even-tempered[11] Slater-type orbitals (see Table I), which are expected to yield results of comparable accuracy for a large range of separations. For Al we have scaled the parameters given by Raffenetti[12] by the factor[13] $\alpha \to \alpha\beta^{1/2}$; this procedure improves the overall consistency of our calculations but slightly decreases the accuracy of the asymptotic energy, as shown in Table I. For the two-center calculations ($R > 2$ a.u.), the sets were expanded by the addition of (a) diffuse ($\alpha\beta^0$) s and p functions

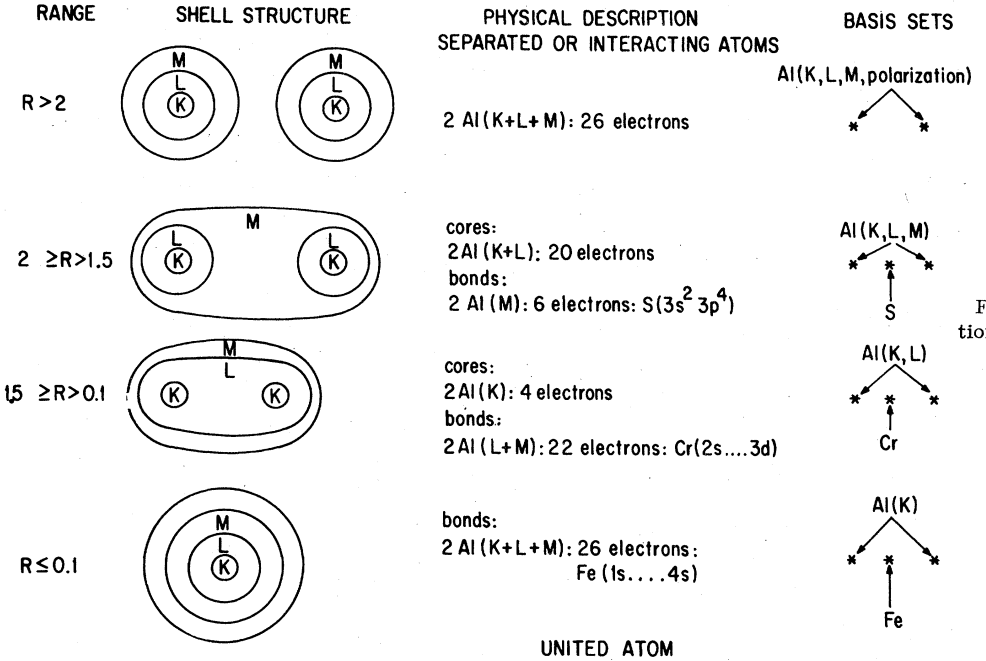

FIG. 1. Basis-set selection scheme. Range in a.u.

TABLE I. Basis sets.

Atom	Energy (in a.u.) Nominal[a]	Even-tempered	Scaled even-tempered parameters[b]	
Al(^2P)	−241.876 52	−241.870 12[c]	α_s	0.662 17
		−241.845 36[d]	β_s	1.726 08
			α_p	0.645 27
			β_p	1.991 73
S(^3P)[e]	−397.504 54	−397.494 46[c]	α_s	0.739 19
			β_s	1.841 12
			α_p	0.662 10
			β_p	2.028 80
Cr(^5D)	−1043.308 90	−1043.367 96[c]	α_s	0.352 32
			β_s	1.697 94
			α_p	1.641 46
			β_p	1.686 89
			α_d	1.178 14
			β_d	2.208 74
Fe(^5D)	−1262.442 50	−1262.358 26[c]	α_s	0.450 45
(^1S)		−1262.002 45	β_s	1.659 25
			α_p	1.679 75
			β_p	1.685 22
			α_d	1.399 41
			β_d	2.083 42

[a] Reference 14.

[b] Double-ζ expansions augmented by one diffuse orbital for each l value. ($\zeta_i = \alpha\beta^i$; $i = 0$ to $2n$).

[c] Corresponds to unscaled parameters.

[d] Corresponds to scaled parameters.

[e] Used in conjunction with Cr d-orbital parameters.

and (b) one f-type and two d-type polarization functions, which were partially optimized at R_e. Following the procedure described by Ermler *et al.*,[5] we employed full double-ζ as well as diffuse $\alpha\beta^0$ functions as bond functions (Fig. 1). For S, standard parameters[12] were used; for Cr and Fe, even-tempered expansions were matched to the nominal basis sets of Wahl *et al.*[14] (Table I).

Errors in the SCF calculation can arise from three sources: the selection of the ground-state configuration, deficiencies in the basis set (expansion error) and correlation error. The first of these will be described in Sec. III. A measure of the expansion error is given by the discontinuities[15] in the potential curve at the points at which the midpoint ("bond") functions are changed. There are three such points in our calculations: $R = 2$ a.u. (from two to three centers, sulfur semiunited atom); $R = 1.5$ a.u. (sulfur to chromium semiunited atom) and $R = 0.1$ a.u. (chromium to iron united atom). Note that most of the region of interest is therefore described by the same basis set, with chromium-bond functions. To estimate the magnitude of the discontinuity, calculations were performed at $R = 1.5$ a.u. with the sulfur basis set and at 0.2 a.u. with the iron basis set. At 0.2 a.u. the calculated total energy difference is 0.08 a.u. (0.01% of the interaction energy); at 1.5 a.u. the corresponding value if 0.07 a.u. (0.7% of the interaction energy). Clearly, the basis sets are sufficiently saturated so that discontinuities in the potential curves which result from basis-function changes are negligible. These discontinuities are generally considerably smaller than differences between the energies of different electronic states (see Sec. III).

The correlation error is also not expected to be large. The atomic correlation energy for transition elements is not available to the best of our knowledge.[16] However, for Fe one may use as a lower bound the value for Ar (Ref. 17): −0.692 a.u.; if we assume a correlation energy of 1 eV/electron in the $3d$ shell, the total correlation energy for Fe is ~0.91 a.u. The correlation energy for Al is −0.488 a.u. The difference in correlation energy between the separate- and the united-atom limit is therefore at most ~0.1 a.u., which is small compared to the potential in the range we shall be concerned with. Therefore, although correlation is quite important for $R \sim R_e$, one can safely neglect it at short range. A relativistic correction comes into consideration for distances smaller than 0.1 a.u. Values for Fe and Al are, respectively, 8.5 and 0.4 a.u.[18] However, even a

correction of 8 a.u. would shift the SCF potential by only 0.7% at $R = 0.1$ a.u.

In the construction of the interatomic potential, we have selected the lowest-energy state at each separation. Our results therefore incorporate the effect of electron jumps from orbitals that correlate with excited (Fe) orbitals to lower-lying orbitals. Figure 2 shows a schematic correlation diagram for Al_2 with the atomic (Fe, Al) orbital energies plotted to scale. The two-electron jumps required for ground-state to ground-state connection are indicated. For example, when the $4\sigma_u$ orbital becomes higher in energy than the half-empty $2\pi_u$, an electron pair jumps into the π orbital, which leads to a filled $3p$ shell in Fe. The crossings are, with one exception, between states of different symmetry, as shown in the following section.

The SCF calculations were carried out with the ALCHEMY series of programs[19]; LCAO calculations to separate core-overlap and valence-electron contributions were performed with the BISONMC programs[14] and are described in detail in Sec. III C.

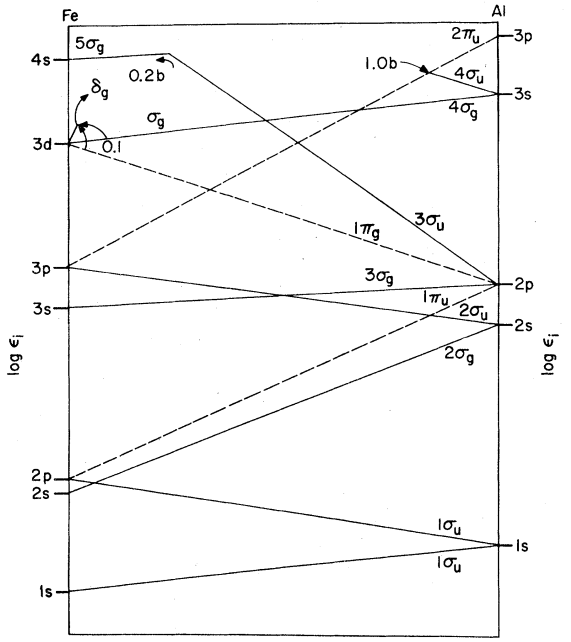

FIG. 2. Correlation diagram for Al_2 (schematic).

III. RESULTS AND DISCUSSION

A. Al-Al potential curves

The ground state of the Al_2 molecule has a $^3\Sigma_g^-(3p\pi_u^2)$ configuration, a dissociation energy $D_e = 1.99 \pm 0.22$ eV and an equilibrium separation $R_e = 4.84$ a.u.[20] However, the SCF ground state, $^3\Pi_u(3p\sigma_g 3p\pi_u)$, does not have the correct symmetry and becomes repulsive much faster than the true ground state as the separation is decreased. For the purpose of extending the SCF potential curves to short range, the true ground state will be taken as the reference state (cf. Table II).

The configurations considered in the present study are listed in Table III. For each configuration, the number of closed shells and partially filled shells of each symmetry are indicated. In each case, only the state with highest multiplicity is considered. The first group of states (group I) in Table III corresponds to the diagonal double excitations associated with the level crossings in Fig. 2; these excitations give rise to one state with the same symmetry as the ground state and to two closed-shell states. Note that the $^1\Sigma_g^+$* state already has the electronic arrangement of Fe ($3d^6$). The $^5\Pi_g$ state (bottom line) corresponds to the first of a series of rearrangements of the $3d$ elec-

TABLE II. SCF energies (in a.u.) for $^3\Sigma_g^-$ state.

R (a.u.)	Two-center calculation	Three-center calculation (sulfur-bond functions)	$V(R)$ [a]
5.0	−483.712 02		−0.0213
4.8	−483.713 89		−0.0232 [b]
4.0	−483.690 97		−0.0025
3.0	−483.428 64	−483.410 15	0.2621
2.0	−482.217 30	−482.389 24	1.3015
1.5	c	−478.568 68	d

[a] Corresponds to the lower of the values in columns 2 and 3.

[b] $D_e = 0.073$ (expt); 0.040 [from CI calculation by M. Leleyter and P. Joyes, J. Phys. Radium 35, L85 (1974)].

[c] Does not converge.

[d] Ground state has different configuration.

TABLE III. Configurations of Al_2 at short range.

Comment	State	Sequence of ground states[a]	Number of closed shells σ_g	σ_u	π_u	π_g	Occupancy of open shells σ_g	σ_u	π_u	π_g	δ_g	Electron transfer[b]
Equilibrium ground state	$X^3\Sigma_g^-$	1	4	4	1	1	0	0	2	0	0	
Group-I excitations	$^3\Sigma_g^-$		5	3	1	1	0	0	2	0	0	$3s\sigma_u^2 \rightarrow 3p\sigma_g^2$
	$^1\Sigma_g^+$	4	4	3	2	1	0	0	0	0	0	$3s\sigma_u^2 \rightarrow 3p\pi_u^2$
	$^1\Sigma_g^+$	5	5	2	2	1	0	0	0	0	0	$2p\sigma_u^2 \rightarrow 4s\sigma_g^2$
												$3s\sigma_u^2 \rightarrow 3p\pi_u^2$
Group-II excitations	$^3\Pi_g$		4	3	1	1	0	1	3	0	0	$3s\sigma_u \rightarrow 3p\pi_u$
	$^5\Sigma_u^-$	2	4	3	1	1	1	1	2	0	0	$3s\sigma_u \rightarrow 3p\sigma_g$
	$^3\Pi_u$		4	3	1	1	1	0	3	0	0	$3s\sigma_u^2 \rightarrow 3p\sigma_g, 3p\pi_u$
	$^3\Sigma_u^+$	3	4	2	2	1	1	1	0	0	0	$3s\sigma_u^2 \rightarrow 3p\pi_u^2$
												$2p\sigma_u \rightarrow 4s\sigma_g$
United atom limit (apart from d-shell rearrangements)	$^5\Pi_g$	6	4	2	2	0	1	0	0	3	2	$3d\sigma_g, 3d\pi_g \rightarrow 3d\delta_g$
												$3s\sigma_u^2 \rightarrow 3p\pi_u^2$
												$2p\sigma_u^2 \rightarrow 4s\sigma_g^2$

[a] The order in which ground-state configurations occur as R is decreased.

[b] With respect to equilibrium ground state $X^3\Sigma_g^-$. Orbital labels correspond to asymptotic Al origin, except for Fe $4s$ and $3d$.

trons in $^1\Sigma_g^+$* required to generate the ^5D term of the Fe manifold. The second group (II) of excitations in Table III represents the single, triple, and split-shell double excitations that can be obtained from the ground-state configuration by removing electrons from the two highest σ_u orbitals, which do not correlate with ground-state Fe, and placing them in either of the orbitals suggested by Fig. 3: $5\sigma_g$ (Fe $4s$) or $2\pi_u$ (Fe $3p$).

Starting at small separations, we have followed the configurations of group I until their energies become higher than those of the group-II configurations; the SCF total energies obtained at various separations are given in Table IV. Several points are worth noting here. First, the present calculations do not include the effects of configuration interaction (CI). CI is expected to have only a small effect on the total interaction energy, but may affect the small separations between states. It will lower the energy of configurations with electron pairs more than that of configurations with unpaired valence electrons (group I over group II). Second, one expects strong interactions between the two sets of $^3\Sigma_g^-$ and $^1\Sigma_g^+$ states, which are close in energy (group I), whereas for group II, states of the same symmetry involve excitations into repulsive orbitals. Thirdly, the total energy of the ground state $E_0(R)$ and the interatomic potential $V(R) = E_0(R) - E(\infty)$ are well approximated by the values that correspond to the group-I configurations at all separations $R \lesssim 1.5$ a.u. This is demonstrated in Table V, which lists interatomic potentials derived from (a) the *ground-state* energies given in Table IV, (b) the energy of the lowest-

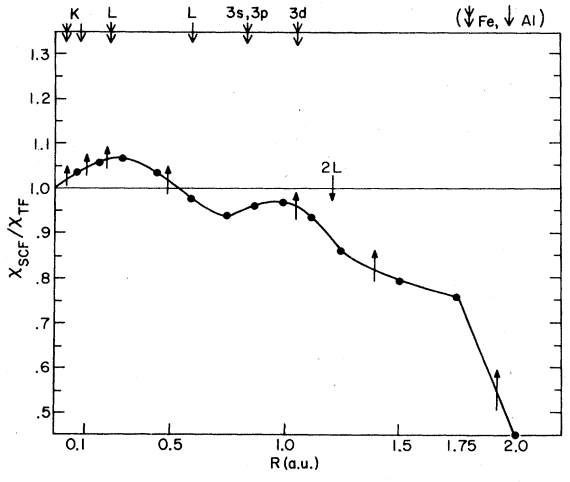

FIG. 3. Ratio of the SCF and TF screening functions for Al_2. Arrows at the top of the figure indicate orbital radii and those that cross the curve indicate changes in electronic configuration.

TABLE IV. Total energy for different states of Al_2 at close range (in a.u.).

R	$^3\Sigma_g^-$	$^5\Sigma_u^-$	$^3\Pi_g$	$^3\Pi_u$	$^3\Sigma_g^{-*}$	$^3\Sigma_u^+$	$^1\Sigma_g^+$	$^1\Sigma_g^{+*}$	$^5\Pi_g$
2	*−482.389 24*[a]	−482.310 8	−482.317 2	−482.133 14	−481.971 70		−482.218 84	−476.237 35	
1.5	−478.568 68	*−478.766 08*	−478.625 95	−478.189 65	−478.732 53	−476.612 74	−478.721 10	−473.975 51	
1.0		−466.968 7[b]		−467.156 98	−467.142 90	*−467.241 19*	−467.096 50	−467.101 58	
0.75		−449.481 13			−451.956 81	*−452.638 42*	−452.584 05	−452.484 13	
0.6					−430.590 12	*−431.568 30*	−431.544 24	−431.483 69	
0.45						−384.619 67	*−384.655 18*	−384.386 82	
0.3							*−267.527 19*	−267.386 03	
0.2							−62.029 93	*−62.061 47*[c]	−61.316 69
0.1								665.166 48[c]	*664.947 34*[d]

[a] Lowest energy at each separation is italicized.
[b] Convergence was slow because of the rapidly changing nature of the $3s\sigma_u$ orbital.
[c] Based on Cr-bond basis; the value for the Fe-bond basis was −62.145 78 a.u.
[d] Nuclear repulsion Z^2/R> electronic energy of Fe.

lying configuration in group I, and (c) the energy for the $^1\Sigma_g^+$ state. The difference between these potentials is less than 1%.

We turn next to a comparison of the interatomic potential of Al_2 obtained in the present work with other, more approximate theories. In Table VI are presented values of the screening function $\chi = V(R)R/Z^2$ for the SCF potential and for the Thomas-Fermi (TF) theory.[1,2,21] The Firsov expression[2] for the screening length is employed in the determination of the TF values. The ratio of the screening functions given in Table VI is plotted in Fig. 3. One observes that the agreement between SCF and TF is good for $R \lesssim 1$ bohr, whereas the SCF potential deviates widely from the TF potential at larger separations. The L-shell radius R_L(Al) of Al [Table VII][22] is ~0.6 a.u.; therefore the deviation of the SCF potential from the TF potential begins at roughly twice the L-shell radius. Thus, TF theory is a fair approximation to the SCF results at separations at which the Al^{3+} cores interpenetrate, but is unsatisfactory at longer range. This behavior is quite understandable. The charge density of a TF atom decays only algebraically at large distances and is much too large in the region of the valence electrons. Furthermore, the onset of bonding effects as $R \to R_e$ enhances the splitting between χ_{SCF} and χ_{TF}.

At separations smaller than $2R_L$(Al) the curve in Fig. 4 exhibits oscillations. It is plausible to attribute these oscillations to "shell effects" associated with the K and L shells. We note in Fig. 3 that the SCF potential is particularly steep at separations just below $R \sim 1.2$ a.u. ~2 R_L(Al) and $R \sim 0.7$ a.u. ~R_K(Al) + R_L(Al). If shell overlap effects are responsible for the oscillations, one might expect these effects to be reflected also in the core kinetic energy. We have indeed found that the total core kinetic energy is relatively flat in the regions 0.6–1.0 and 1.5–1.75 a.u., which is consistent with the behavior in Fig. 4.

An interatomic potential for Al_2 has been calculated by Wilson, Haggmark, and Biersack[4] based on the density-functional approach referred to in the Introduction. The screening function for this potential is plotted in Fig. 4 along with χ_{SCF} and χ_{TF}. The WHB and SCF screening functions both begin to deviate from the TF curve for $R \gtrsim 1$ a.u. The SCF curve exhibits a "kink" near $R = 2$ a.u. This kink is most likely associated with the changes in electronic structure that occur in this region (see Sec. III B); several tests were performed to verify that this feature is not an artifact of the basis set employed. The SCF and WHB curves are in good agreement between 2 and 3 a.u. The SCF curve then drops sharply (not shown in Fig. 4) and $V(R)$ becomes negative at 4 a.u. (Table II).

TABLE V. Potential energy[a] (in a.u.).

R (a.u.)	Ground state	$V(R)$	$V_1(R)$[b]	Percent change[c]	$V_2(R)$[d]	Percent change[c]
2.0	$^3\Sigma_g^-$	1.3015	1.3015	...	1.3015	...
1.5	$^3\Sigma_g^{-*}$	4.925	4.958	0.7	4.970	0.9
1.0	$^3\Sigma_u^+$	16.449	16.548	0.6	16.594	0.9
0.75	$^3\Sigma_u^+$	31.052	31.107	0.2	31.107	0.2
0.6	$^3\Sigma_u^+$	52.122	52.146	0.05	52.146	0.05
0.45	$^1\Sigma_g^+$	99.036	99.036	...	99.036	...
0.3	$^1\Sigma_g^+$	216.163	216.163	...	216.163	...
0.2	$^1\Sigma_g^{+*}$	421.545	421.545	...	421.661	...
0.1	$^5\Pi_g$	1148.64	1148.86	0.02	1148.86	0.02

[a] $V(R)=E_0(R)-E(\infty)$; $E(\infty)=-483.69072$ a.u.
[b] $V_1(R)=E_1(R)-E(\infty)$, where E_1 corresponds to the lowest-energy group-I configuration.
[c] With respect to $V(R)$.
[d] $V_2(R)=E_2(R)-E(\infty)$, where E_2 is the energy of the $^1\Sigma_g^+$ state.

B. Population analysis, molecular-orbital correlation diagrams, and total charge densities

In the three-center approach adopted in the present study, the number of basis functions centered on the Al atom is reduced as the interatomic separation is decreased. On the other hand, the number of basis functions centered on the midpoint between the Al atoms is kept relatively constant. This procedure results in a transfer of charge from the atomic bases to the midpoint bases as the internuclear distance is decreased. Figure 5 shows Mulliken total populations on the two Al atoms (broken line) and on the bond for the $^1\Sigma_g^+$ state. As discussed above, the energy of this state is close to the ground-state energy at separations $\lesssim 1.5$ a.u. As one observes in Fig. 5, a gradual buildup occurs in the charge associated with the bond until a separation close to the L-shell radius of Fe is reached; for smaller separations the united-atom character is manifested by a rapid increase in the bond population.

A correlation diagram for several orbitals of Al_2 is plotted in Fig. 6. The labels on the right-hand side indicate the Al parentage. The $2\sigma_g$ orbital (Al $2s$ – Fe $2s$) approaches the united-atom limit smoothly; this behavior is also observed for the $1\sigma_g$ orbital, which is not represented in the figure. In general, the correlation diagram in Fig. 6 is considerably more complicated than the schematic one shown in Fig. 2. Some of the finer structure in the curves may be due to basis-set deficiencies; this question could be investigated with numerical Hartree-Fock methods.[23]

Calculations of total electronic charge density

TABLE VI. SCF and Thomas-Fermi screening functions $\chi(x)$ for Al_2.[a]

R (a.u.)	$x=R/a$[b]	χ_{TF}	χ_{SCF}	χ_{SCF}/χ_{TF}
2.0	8.432	0.033	0.015	0.45
1.5	6.324	0.055	0.044	0.799
1.25	5.270	0.073	0.062	0.851
1.0	4.216	0.101	0.097	0.964
0.75	3.162	0.147	0.138	0.939
0.60	2.530	0.190	0.185	0.974
0.45	1.897	0.255	0.264	1.035
0.30	1.265	0.360	0.384	1.067
0.20	0.843	0.471	0.499	1.059
0.10	0.422	0.656	0.680	1.037

[a] $\chi=V(R)R/Z^2$, where $Z=13$.
[b] $a=0.8853/(Z^{1/2}+Z^{1/2})^{2/3}=0.2372$.

TABLE VII. Radial expectation values $\langle R_{nl}\rangle$ (a.u.) for atomic orbitals.[a]

	Al	S	Cr	Fe
$1s$	0.12	0.10	0.06	0.06
$2s$	0.62	0.48	0.29	0.27
$3s$	2.60	1.72	0.91	0.82
$4s$			3.48	3.24
$2p$	0.60	0.44	0.26	0.24
$3p$	3.43	2.06	0.97	0.87
$3d$			1.22	1.07

[a] Reference 19.

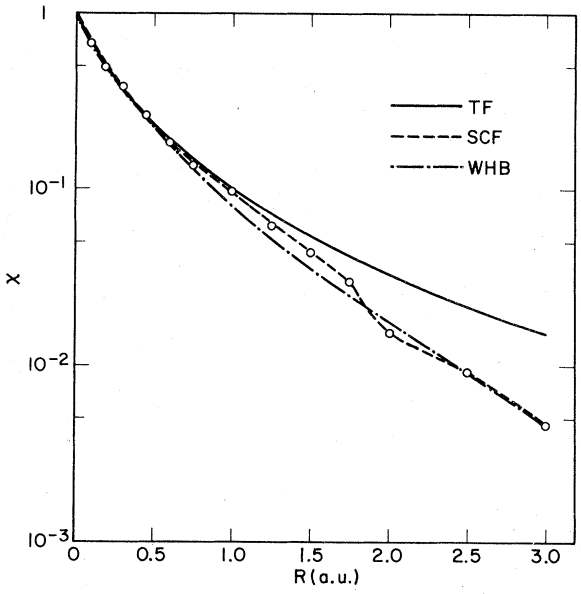

FIG. 4. Screening functions for Al_2.

at the midpoint between the Al atoms have been performed. The results are shown in Table VIII along with values obtained by superposition of atomic charge densities. The ratio of the SCF to the superposed charge densities is plotted in Fig. 7. As expected, positive deviations from superposition (a ratio greater than unity) occur in the vicinity of R_e, whereas negative deviations occur at smaller separations as a result of the exclusion principle. As the internuclear separation becomes still smaller ($R<2$ a.u.), the ground-state electronic configuration changes (Tables III and IV). One observes in Fig. 6 that at close separations the antibonding $3s\sigma_u$ and $2p\sigma_u$ orbitals are vacated in favor of the bonding $3p\pi_u$ and $4s\sigma_g$ orbitals. As

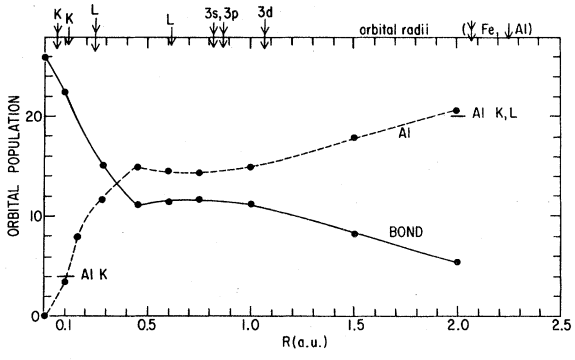

FIG. 5. Total Mulliken orbital populations for $^1\Sigma_g^+$ state.

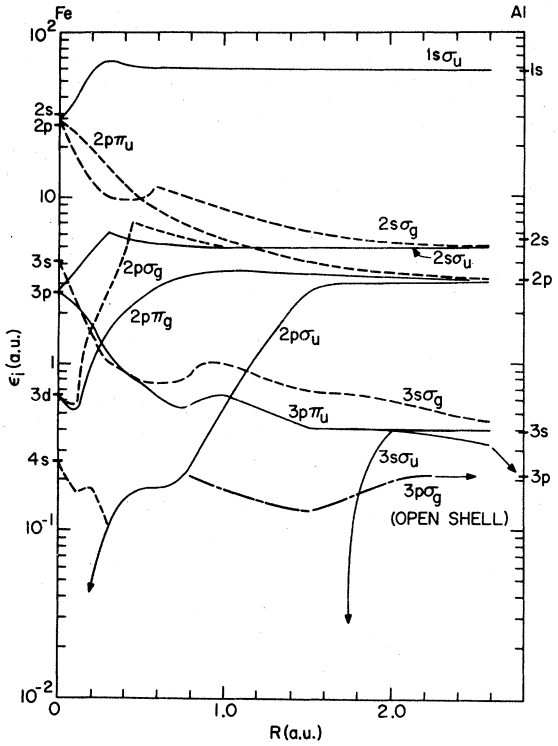

FIG. 6. Correlation diagram for Al_2.

a result of these changes in configuration, a transfer of electronic charge back to the midpoint region occurs. The buildup of charge is quite pronounced at 1 a.u.: 17 electrons in bonding (σ_g, π_u) orbitals and 9 in antibonding (σ_u, π_g) ones, as compared with 15 and 11 electrons, respectively, at 1.5 a.u. and 14 and 12 electrons at 2.0 a.u. (Table III). This electron promotion and the resultant redistribution of charge are most likely responsible for the kink observed in the screening function (Fig. 4) just below 2 a.u.[24]

C. Decomposition of total energy into core and valence contributions

We consider here the separate contributions to the interatomic interaction from core and valence electrons. Such a decomposition has been studied previously on the basis of more approximate theories.[7,8] To determine the core contributions to the interatomic potential within the SCF framework, several types of calculations were performed with the valence electrons omitted[25] (see Table IX). First, the total energy of Al_2^{6+} was calculated using an LCAO method; the atomic orbitals employed were (a) even-tempered orbitals[12] for Al^{3+} (LCAO-IO) and (b) core orbitals obtained from the SCF calculations for the ground-

TABLE VIII. Total electronic charge density at midpoint position as a function of separation.

	R (a.u.)					
	1.0	1.5	2.0	3.0	4.0	5.0
Al_2	8.5628	1.9726	0.4920	0.0886	0.0543	0.0272
2Al	7.9591	2.1139	0.5290	0.0764	0.0375	0.0204
Al_2, core	8.2785	1.9402	0.4884	0.0362	0.0021	0.0000
$2Al^{3+}$	7.9786	2.1124	0.5159	0.0322	0.0020	0.0000

state configuration of (neutral) Al_2 (LCAO-MO). The core overlap interaction is defined by

$$\Phi_{0I}(R) = V(R) - Z_v^2/R ,$$

where $Z_v = 3$ and $V(R) = E_{\mathrm{LCAO}}(R) - E(\infty)$. Here $E(\infty) = -479.936\,82$ a.u. is the value appropriate to the even-tempered Al^{3+} basis set. The third set of values in Table IX refers to SCF calculations for Al_2^{6+}. These energies are lower than those obtained in the LCAO-MO calculation because polarization of the ion cores occurs in the SCF calculations. In the last column of Table IX we list values of Φ_{0I} calculated with the Gordon-Kim (GK) program.[8,26] The method of GK is essentially the same as that of WHB.[4] In the present calculations with the GK program, the electron densities correspond to the even-tempered basis for Al^{3+}. Figure 8 shows core-overlap interactions Φ_{0I} obtained with the GK method for several diatomic systems. The values for systems other than Al_2 were taken from the second paper cited in Ref. 8. The small value of Φ_{0I} for Al_2 reflects the relatively small atomic core size of Al. The triangles in the figure denote the LCAO-MO results. For $R \lesssim 2$ a.u. the GK values are slightly lower than those of the LCAO-MO calculations, as one can also verify in Table IX. The differences may to some extent be due to the neglect of gradient terms[27] and to the superposition approximation in the GK calculation (see Fig. 7).

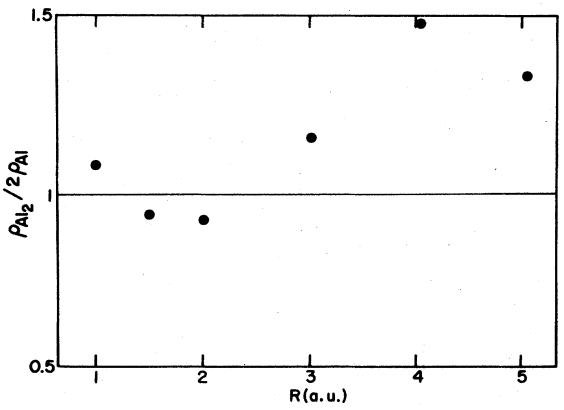

FIG. 7. Ratio of SCF charge density to superposed atomic charge densities at midpoint between Al atoms.

The core-overlap interaction obtained with the LCAO-MO method is plotted along with the total SCF potential $V(R)$ (Table V) in Fig. 9. One observes that core overlap becomes the dominant contribution to $V(R)$ (i.e., greater than half) for separations $\lesssim 1.5$ a.u. At larger separations the interatomic forces are dominated by the combined effects of the valence electrons and the Coulomb repulsion Z_v^2/R. The latter two contributions, of course, are of opposite sign and cancel each other to a large extent.

The values of Φ_{0I} obtained from the LCAO-MO calculation are lower than those obtained earlier by one of us[7] using the Heitler-London method. The former method is clearly the more accurate one in principle; at large separations, however, the LCAO-MO method may become inaccurate because Φ_{0I} is expressed as a small difference between large numbers. At a separation of 3 bohr the LCAO-MO value is negative whereas the GK, LCAO-IO, and Heitler-London values[7] are positive. To check the adequacy of the basis set at this separation, the LCAO-MO calculation was repeated using the Bagus-Gilbert[20] nominal set. The result, $\Phi_{0I} = -0.0083$ a.u. was essentially similar to that obtained with the even-tempered basis. Additional checks revealed that the negative value of Φ_{0I} is associated with core polarization; if the polarization functions are removed from the basis sets, a positive value of Φ_{0I} is obtained at 3 a.u.

D. Interaction between Al and Al^{3+}

One of the goals of the present study was to obtain a potential appropriate to energetic Al atoms in Al metal. It is important to recognize that a fast particle in matter is normally ionized; the extent of ionization depends on its velocity. Therefore, the neutral-atom potentials described thus

TABLE IX. Core-overlap interaction[a] Φ_{0l} for Al_2.

R (a.u.)	LCAO[b] MO: core orbitals taken from SCF calculations for Al_2 three-center	LCAO[b] MO: core orbitals taken from SCF calculations for Al_2 two-center	IO: even-tempered ionic orbitals two-center	Self-consistent field (Al^{6+}) three-center	Self-consistent field (Al^{6+}) two-center	Gordon-Kim even-tempered ionic orbitals
5		0.0019	0.0001		−0.0089	
4		0.0027	0.0003		−0.0190	
3		−0.0225	0.0028		−0.0429	
2	0.2486	0.1575	0.255	0.178	0.123	0.19
1.5	1.988		1.990	1.965		1.44
1.0	13.309		13.64	12.340		9.26
0.75	25.999		34.38	25.801		23.30
0.6	44.713		61.37	44.531		42.81
0.45	93.026		118.12	87.713		85.58
0.3	198.147		247.08	197.726		195.23
0.2	388.028		446[d]	387.222		392.78
0.1			1500[d]	1072.14		1083.65

[a] Total energy is calculated for Al_2^{6+}; the valence electrons are omitted.
[b] Linear combination of (previously determined) orbitals.
[c] Aluminum basis sets reduced at smaller separations as indicated in Fig. 1.
[d] Basis sets too small to provide meaningful results.

far are not strictly appropriate to ion–neutral-atom interactions. Unfortunately, the SCF and LCAO methods are not immediately applicable to such interactions. Nevertheless, one can estimate the energy of the ion–neutral-atom system by expressing atomiclike orbitals in terms of molecular orbitals. For example, localized orbitals on atom A of diatomic aluminum can be ex-

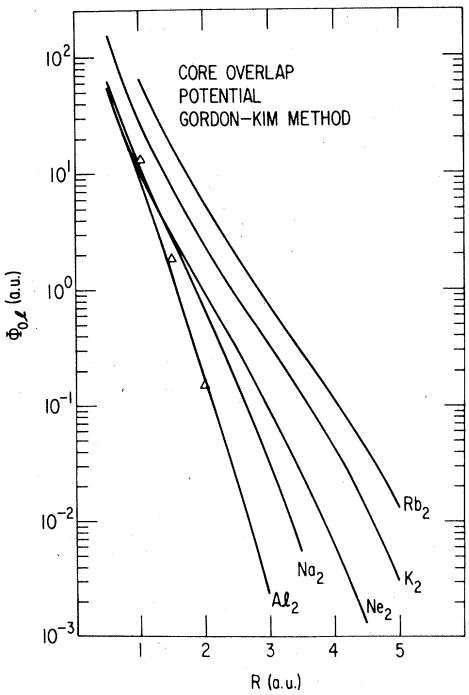

FIG. 8. Core-overlap potential calculated for several diatomic systems with the Gordon-Kim method. The triangles denote LCAO-MO results for Al_2.

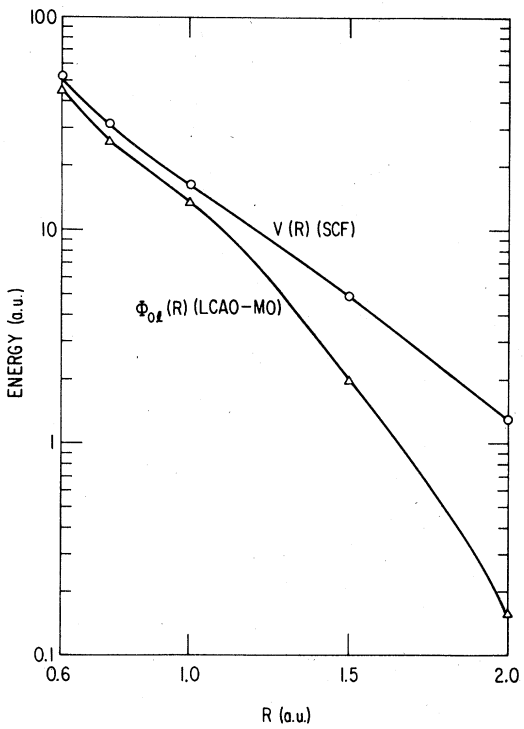

FIG. 9. Core-overlap potential and SCF potential for Al_2.

TABLE X. Interactions[a] between Al and Al^{3+}.

R (a.u.)	Al^{3+}-Al^{3+} SCF[b]	Al-Al^{3+} LCAO-MO $^2\Pi$	Al-Al SCF[c]
5	1.791	−0.0023[d]	−0.0148
4	2.231	0.2201[d]	−0.0025
3	2.957	1.0301[d]	0.2621
		1.298	
2	4.678	4.073	1.3015
1	21.340	19.475	16.449
0.75	37.801	34.811	31.052
0.3	227.726	221.561[e]	216.163

[a] $V(R)$ in a.u.; the asymptotes are as follows: $E_{Al_2}(\infty)$ = −483.690 72 a.u.; $E_{Al_2^{3+}}(\infty)$ = −481.813 77 a.u.; $E_{Al_2^{6+}}(\infty)$ = −479.936 82 a.u.

[b] Values given in Table IX plus Z_v^2/R.

[c] Values given in Table V.

[d] Weighted average of all six states.

[e] Lowest state only; average = −235.167 a.u.

pressed as

$$3s_A = 4\sigma_g + 4\sigma_u\,,$$
$$3p_A = 2\pi_u + 2\pi_g \text{ or } 3p_A = 3\sigma_g + 3\sigma_u\,, \tag{3.1}$$

where the molecular σ and π orbitals can be obtained from either SCF or LCAO states. The asymmetric "molecular" state

$$\Psi_{\pi_A} = (Al_2^{6+}\ \text{core})3s_A 3\bar{s}_A 3p_A\,,$$

which corresponds to the system Al-Al^{3+}, can be written in terms of (proper) molecular states by use of Eq. (3.1):

$$\begin{aligned}\Psi_{\pi_A} = {} & 4\sigma_g^2 2\pi_u + 4\sigma_g^2 2\pi_g + 4\sigma_u^2 2\pi_u + 4\sigma_u^2 2\pi_g \\ & + (4\sigma_g 4\bar{\sigma}_u + 4\bar{\sigma}_g 4\sigma_u)2\pi_u \\ & + (4\sigma_g 4\bar{\sigma}_u + 4\bar{\sigma}_g 4\sigma_u)2\pi_g\,.\end{aligned} \tag{3.2}$$

The energy of the state Ψ_{π_A} is the appropriate average of the energies of the six states given in Eq. (3.2). Table X presents numerical results for this calculation. The energies of the six molecular states were obtained by LCAO-MO calculations based on orbitals generated in the SCF calculations for Al_2. Only the $^2\Pi$ state was considered since the $^2\Sigma$ state (i.e., $\Psi_\sigma = 3s_A^2 3p\sigma_A$) is higher in energy at 4 a.u. and, as expected, rises more steeply with a decrease in R.

For $R < 3$ a.u., the average of the two states with three open shells [i.e., the last two states given in Eq. (3.2)] reproduces the full results very well. This latter approximation was employed to circumvent difficulties associated with the $3s\sigma_u$ orbital description (see Fig. 6).

The energies for the Al-Al^{3+} interaction are plotted in Fig. 10. The SCF potentials for Al_2

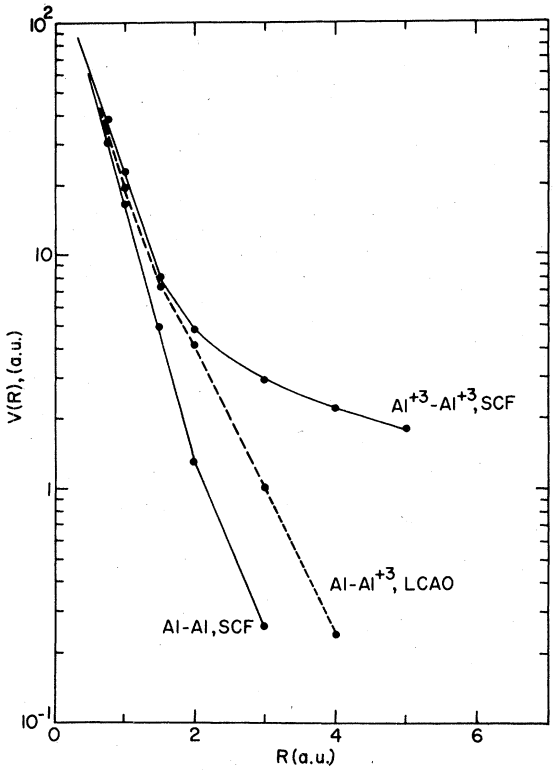

FIG. 10. Al-Al, Al-Al^{+3}, and Al^{+3}-Al^{+3} interactions.

(Table V) and Al_2^{6+} are given for comparison. The Al-Al^{3+} and Al_2 potentials and their derivatives are quite similar for $R \lesssim 1$ a.u.

IV. CONCLUSIONS

The short-range interaction between two aluminum atoms has been studied by SCF techniques. A three-center expansion based on Slater-type orbitals with even-tempered exponents was employed. S, Cr, or Fe exponents were used at the central expansion point, depending on the interatomic separation. This procedure yielded a smooth potential with negligible discontinuity at the points at which the basis set was changed.

The following sequence of ground states was observed as the separation was decreased.

$$^3\Sigma_g^- \rightarrow {}^5\Sigma_u^- \rightarrow {}^3\Sigma_u^+ \rightarrow {}^1\Sigma_g^+ \rightarrow {}^1\Sigma_g^+ \rightarrow {}^5\Pi_g\,.$$

Certain states (designated as group I) such as $^1\Sigma_g^+$ give a good approximation to the ground-state energy at all separations < 1.5 a.u.

The SCF potential is in good agreement with TF for separations smaller than ~1 a.u. A similar result was found previously for AlH.[3] At larger separations the SCF potential decreases more rapidly than TF, and it becomes negative between 3 and

4 a.u. The SCF potential is in reasonable overall agreement with the density-functional calculations of WHB.[4] A kink is observed in the SCF screening function at a separation near $R = 2$ a.u. This behavior is most likely related to the changes in the ground-state configuration that occur in this vicinity.

The contribution of core overlap to the interatomic potential was estimated from LCAO calculations in which the valence electrons were omitted. Core overlap becomes the dominant contribution for separations $\lesssim 1.5$ a.u.

ACKNOWLEDGMENTS

The authors are indebted to Dr. R. C. Raffenetti for the ALCHEMY-BISON interface.

This work was supported by the U.S. Department of Energy.

---

*Visiting scientist from the University of Illinois at Chicago Circle.

†Present address: Environmental Impact Studies Division, Argonne National Laboratory.

[1]J. Lindhard, V. Nielsen, and M. Scharff, K. Dan. Vidensk. Selsk. Mat.-Fys. Medd. 36, 10 (1968).

[2]O. B. Firsov, Sov. Phys. JETP 5, 1192 (1957); 6, 534 (1958); 9, 1076 (1959).

[3](a) See, e.g., P. Gombas, in *Encyclopedia of Physics* (Springer, Berlin, 1956), Vol. 36; (b) G. Moliere, Z. Naturforsch. A 2, 133 (1947).

[4]W. D. Wilson, L. G. Haggmark, and J. P. Biersack, Phys. Rev. B 15, 2458 (1977).

[5](a) J. S. Briggs and M. R. Hayns, J. Phys. B 6, 514 (1973); (b) W. C. Ermler, R. S. Mulliken, and A. C. Wahl, J. Chem. Phys. 66, 3031 (1977).

[6]N. H. Sabelli, M. Kantor, R. Benedek, and T. L. Gilbert, J. Chem. Phys. 68, 2767 (1978).

[7]R. Benedek, Phys. Rev. B 15, 2902 (1977).

[8]R.G. Gordon and Y. S. Kim, J. Chem. Phys. 56, 3122 (1972); Y. S. Kim and R. G. Gordon, *ibid.* 60, 1842, (1974); 60, 4323 (1974).

[9]U. Fano and W. Lichten, Phys. Rev. Lett. 14, 627 (1965).

[10]R. G. Parr, Proc. U. S. Natl. Acad. Sci. 12, 763 (1975); P. Politzer, J. Renther, and G. T. Kasten, J. Chem. Phys. 67, 2383 (1977).

[11]K. Ruedenberg, R. C. Raffenetti, and R. D. Bardo, in *Energy Structure and Reactivity, Proceedings of the 1972 Boulder Research Conference on Theoretical Chemistry,* edited by D. W. Smith (Wiley, New York, 1973), p. 164.

[12]R. C. Raffenetti, J. Chem. Phys. 59, 5936 (1973).

[13]R. C. Bardo and K. Ruedenberg, J. Chem. Phys. 59, 5966 (1973); T. H. Dunning, Jr., *ibid.* 53, 2823 (1970).

[14]A. C. Wahl, P. J. Bertoncini, K. Kaiser, and R. H. Land, BISON: Argonne National Laboratory Report No. ANL-7271, 1968 (unpublished); G. Das and A. C. Wahl, BISON-MC: Argonne National Laboratory Report No. ANL-7955, 1972 (unpublished).

[15]The discontinuities could be eliminated (or smoothed out) by scaling the basis-function exponents continuously from the values for S to those for Fe as a function of R.

[16]Only the influence of electron correlation on selected properties has been considered [see, for instance, C. Froese-Fischer, J. Phys. B 10, 1241 (1977)].

[17]A. Veillard and E. Clementi, J. Chem. Phys. 49, 2415 (1968).

[18]S. Fraga, J. Karwoski, and K. M. S. Saxena, *Handbook of Atomic Data* (Elsevier, New York, 1976).

[19]P. S. Bagus, B. Liu, A. D. McLean, and M. Yoshimine (private communication); P. S. Bagus, IBM Technical Report No. RJ 1077, 17873, 1972 (unpublished).

[20]D. S. Ginter, M. L. Ginter, and K. K. Innes, Astrophys. J. 139, 365 (1964); *International Tables of Constants and Numerical Data, Spectroscopic Data Relative to Diatomic Molecules* (Pergamon, New York, 1970), Vol. 17.

[21]S. Kobayashi, T. Matsukuma, S. Nagai, and K. Umeda, J. Phys. Soc. Jpn. 10, 759 (1955).

[22]P. S. Bagus, T. L. Gilbert, and C. C. J. Roothaan, J. Chem. Phys. 56, 5195 (1972); values from extended tabulations provided by the authors.

[23]E. A. McCullough, Jr. (private communication). Unfortunately, presently available programs can not be used routinely on systems as large as Al_2.

[24]One may consider the SCF screening function to be composed of two distinct parts that correspond to (a) an open-shell molecular system ($R \gtrsim 2$ bohr) and (b) a closed-shell pseudoatomic one ($R \gtrsim 2$ bohr).

[25]At separations below ~ 1 bohr, the distinction between core and valence becomes somewhat arbitrary, as shown in Fig. 6. In the present calculation, the six highest-energy electrons at each separation are considered "valence" electrons; all others are "core" electrons.

[26]S. Green and R. G. Gordon, Q.C.P.E. Program No. 251, POTLSURF, 1973 (unpublished).

[27]C. C. Shih, Phys. Rev. A 14, 919 (1976).